ISSN 1392-1320 MATERIALS SCIENCE (MEDŽIAGOTYRA). Vol. 29, No. 4. 2023

Multi-objective Optimization of Laser Welds with Mixed WC/Co/Ni Experiments Using Simplex-centroid Design

Chao-Yang ZHANG [1], Shenyu CHEN [2], Lin-gjun XIE [1], Echo YANG [1], Tong BU [1], Ivan CHEUNG [1], Ming-Der JEAN [1] *

[1] *College of Arts and Design, Jimei University, 185 Yinjiang Rd., Jimei District, Xiamen,361021, China*
[2] *Venice Academy of Fine Arts, Fondamenta Zattere Allo Spirito Santo,423,30123 Venezia VE, Italy*

https://doi.org/10.5755/j02.ms.33626

Received 13 March 2023; accepted 8 May 2023

This work involves the preparation of WC/Co/Ni blends using different mixing ratios to form Co/Ni/WC composite-based coatings by laser cladding. The effect of each component and their mixtures on the mechanical properties was evaluated using a mixture design approach. The morphologies and microstructures of the laser clads were characterized using a scanning electron microscope and X-ray diffraction techniques. Cracking behavior and fracture based on residual stresses are explored. In addition, the mathematical models between the three-component mixtures and the mechanical properties of the laser clad were established. The results showed that the welds containing 50 % WC-50 % Ni alloys were successfully deposited by laser cladding with favorable mechanical properties. These welds reduced the remarkable fracture crack activities and did not cause delamination in the laser clads. An increase in WC content significantly enhances wear resistance and microhardness, except for the crack susceptibilities in all mixtures. Additionally, when increased Co/Ni on WC, the reduction of adhesive wear is more significant than that of abrasive wear. Wear resistance is improved by the high content of WC particles in the laser-clad joints. Based on the mixture models, better mixed ratios for the blends that were developed using a multi-objective superimposed optimization technique make these blended materials promising candidates and can ensure the quality of laser clads. The findings from this study will greatly contribute to optimizing the blend ratio of the three-ingredient mixture based on mixture design to enhance structural evolution and mechanical properties, and also obtain better quality laser-clad coatings.

Keywords: laser cladding, mixture design, microstructural evolution and mechanical properties, wear resistance.

1. INTRODUCTION

Metal matrix composites are attracting much attention for the hardfacing environment in the form of coatings in industrial applications, which have protective ability against high temperature, wear, corrosion, impact and fatigue, especially applications in cutting tools, turbine blades, engine valves and other fields. Recently, there has been great interest in using ceramic matrix composites on steel and non-ferrous metal alloys, with their comprehensive properties being proven to be excellent protective materials for additive manufacturing [1 – 4]. They are made of metallic matrix reinforced composites with hard alloys including carbides, nitrides and borides [5 – 8]. Among those, ceramic matrix composites have been studied in industrial applications typically comprising hard carbides such as WC, NbC, SiC, which are widely used in metal cutting industries to efficiently improve surface protection against wear, corrosion, and thermal properties [9]. These carbides improve the resistance to wear as effectively as metal matrix composites [10]. Despite having excellent mechanical and thermal properties, several shortcomings have been identified, such as weak reinforcing effects, structural defects, thermal stress concentration and the formation of cracks, especially in the high fraction tungsten carbide coatings [11]. These characteristics are the most important factors affecting the performance of cladding WC reinforced coatings. They reduce the lifetime of industrial components and have difficulty meeting the developed requirements, thereby resulting in large obstacles to their intensive applications in the industry. Accordingly, it is desirable to develop an effective manufacturing method to solve the technical barriers of laser-clad WC welds.

Recently, several studies have examined the hardfacing activity of WC deposits by powder-based additive manufacturing techniques, which are capable of producing complex geometries close to their net-shape using ceramic materials. Due to its dense features, good metallurgical bonding to substrate, lower distortion and porosity, as well as manufacturing flexibility and ease of automation, laser cladding has received considerable attention as a promising powder-based technology for protective coatings [12]. Laser cladding with superior properties that were previously unachievable has several advantages over conventional hardfacing techniques. Accordingly, this technique is of utmost importance in this additive manufacturing field. Although studies show much research on metal matrix composites with Ni/Co additives improving the vulnerability problems of WC reinforced coatings during laser cladding, no reports of these mixed powders by laser cladding were found by statistical mixture design.

* Corresponding author. Tel.: +0592-6181815; fax: +0592-6180809.
E-mail: *202261000183@jmu.edu.cn* (M.D. Jean)

For laser clads, available publications mainly focused on describing the metal matrix coatings, whereby WC-based alloys are usually doped in the metal matrix by adding coating materials as metal binder alloys to form the ceramic-matrix composite clads and improve the microstructure and mechanical properties of WC reinforced composite coatings [13, 14]. However, high hardfacing clads have several drawbacks during the cladding processes, such as high residual stress, pores, cracks, distortion and delamination problems. Therefore, there are significant challenges in attaining WC reinforced composite coatings to retain the integrity of WC reinforced composites that show a favorable microstructure and effective properties in wear environments. To overcome the aforementioned problems, many researchers have looked into developing various methods to deal with difficult-to-process metal matrix composites, especially in the WC reinforced composite coatings. However, most investigators concentrated on improving laser-clad WC reinforced composites during laser cladding and many studies have reported that metallic binders are added to WC to solve several harmful problems of highly brittle WC coatings [15]. This has the advantage of enhancing the strength of the WC area due to the doped metal binder. Recent studies on resistant materials in ceramic matrix composites, including WC-Co, WC-Ni, WC-Co-Ni alloys or mixed carbides, showed excellent performance in high wear and corrosion resistive environments, and have received a great deal of attention in industrial applications [16]. The impact of controlling the ratio of mixed powders and mixtures on the mechanical properties of WC/Co/Ni composites is very difficult using the trial-and-error method. In addition, few researchers studied the improvement in mechanical properties of WC reinforced coatings using cladding W/Co/Ni powder blends to form ceramic-matrix composite welds by mixture design, which is a good alternative to solve the mixture problems of metal binder powders including the relationships among the proportions of different components and responses of composite WC/Ni/Co clads [17, 18]. In recent studies, there have been a few concerns regarding the development of a mixture design for the metal binder on WC [19, 20]. This is currently a strong development in the range of new and more efficient additive processes which employ different percentage fractions of WC/Ni/Co blends concentrating on the mechanical properties of a clad. Accordingly, it is important to synthesize mixtures with the proper blend ratio of WC/Ni/Co powders to control the coated performance of composite WC/Ni/Co welds during laser cladding.

The focus of the present work is to apply the mixture of WC, Co and Ni alloys on 45 steel to form ceramic matrix composites by laser cladding [21, 22]. The microstructural evolution, crack formation, and influence of each component and their mixtures on the mechanical properties were systematically studied. Further, a response surface methodology with a simplex-centroid design is utilized. This could assess the effect of each mixture component as well as the interactive effect between different components on each response and their responses on the yields. The quality of a clad in optimizing the weight fractions of three ingredients in the contour plots is further discussed in the WC/Co/Ni welds.

2. EXPERIMENTS

The fiber laser cladding system mainly consists of IPG YLS-3000 fiber laser, six-axis robot, an induction power supply, a computer digital controller and a powder feeder (HUST III). The WC/Ni/Co powder blends were composed of WC and Co/Ni clad powder with sizes of 125 μm to 300 μm. The cladding material used in this study was a mixture of WC with 90 wt.% W and 10 wt.% C. The Co/Ni alloy powders were mixed with the WC alloy powders according to the different weight fractions of the Co, Ni and WC blends. There are three different alloy powders blended to make up the laser clads, in which mixing experiments were used to examine the results obtained for the combination of these components. The substrate metal was 45 steel with dimensions of 40 mm, 20 mm and 10 mm. The working surface was cleaned with absolute ethyl alcohol. The chemical composition of 45# carbon steel: the amount of carbon (C) is 0.42 ~ 0.50 %; Si content is 0.17 ~ 0.37 %; Mn content is 0.50 ~ 0.80 %; Cr content is ≤ 0.25 %; Ni content is ≤ 0.30 %; Cu content is ≤ 0.25 %. The microstructures of the composite WC/Co deposits were examined using a Hitachi S-2600H (Tokyo, Japan) scanning electronic microscope (SEM), and the etching test with a Nital for 5 – 10 s was conducted, and a Tukon 2500 digital microhardness (HV) tester was used. In addition, residual stress analyses were carried out at the bead centerline using an XRD diffractometer (Proto iXRD) with the sin2ψ method, corresponding to $\psi = 0°$ and $\psi = 90°$, respectively, which were acquired by tilting angles of 0°, 15°, 30°, 45° and 60° [23, 24]. A ball-on-block sliding wear tester is used. The wear tests were carried out under applied loads of 20 N. The sliding distance for the test was 1000 m. The speed of friction was 10 mm/s. The data with the control factors and levels in the coded design units are presented in this study, including a laser power of 1.2 kW, stand-off distance of 20 mm, argon gas flow at 10 l/min, feed rate of 1500 l/min and a scanning speed of 8 mm/s, respectively, which were deposited onto the coatings and solidified to form a clad bead.

3.3. EXPERIMENTAL DESIGN AND ANALYSIS

The development of a new product requires optimization procedures to find better processing and control parameters, as well as higher quality and lower costs. Mixture designs act as quality technology to produce excellent products. Two or more components are mixed using many different proportions, and the characteristics of the responses are recorded. Mixture designs, however, can construct several responses to be simultaneously optimized from a ternary mixture proportion is determined. As mentioned in the literature above, it is more difficult to optimize using traditional analytical methods. The laser clad is done with a mixture of three different powders: WC(X_1), Ni(X_2) and Co(X_3) indicating the fraction of the blends is of interest: a mixture of WC, Co and Ni alloys in which the best formation of WC/Co/Ni welds was obtained. It is noted that the proportion of each component in the mixture has its restriction, $X_1 \geq 0$, $X_2 \geq 0$, $X_3 \geq 0$, in the form of $X_1 + X_2 + X_3 = 1$. Based on the analysis above, the simples-

centroid mixture design with a lower-bound constraint on the component proportions was determined as shown in Table 1. The forms of regression model of the three responses such as residual stress behaviors, microhardness levels and wear volume losses of the laser-clad welds were established through Scheffé polynomial regression fitting [25]. The regression equations of the mixture models are presented as follows:

$$\mathbf{E(y)} = \sum_{i=1}^{n} \boldsymbol{\beta}_i \boldsymbol{x}_i + \sum \sum_{i<j=2}^{n} \boldsymbol{\beta}_{ij} \boldsymbol{x}_i \boldsymbol{x}_j + \sum \sum_{i<j<k=3} \sum^{n} \boldsymbol{\beta}_{ijk} \boldsymbol{x}_i \boldsymbol{x}_j \boldsymbol{x}_k \qquad (1)$$

where x_i, x_j and x_k are the levels of the variables; β_i is the coefficient of the linear term; β_{ij} and β_{ijk} are the coefficient of the quadratic terms; *E(y)*is the output and *n* is the number of variables. For example, the formation of WC/Co/Ni by laser cladding is considered. The experimental data adopts a simplex-centroid design, which can detect the effect of each mixture component as well as the interactive effect between different components on each response.

4. EXPERIMENTAL RESULTS AND DISCUSSION

4.1. Microstructural evolution

Fig. 1 shows the SEM morphologies of WC with mixed Co/Ni ratios, where the cross section of the sample is etched and the microstructures of the composites are shown. Due to the different WC content in the molten zone by laser cladding, various carbides such as WC, W_2C and Fe_3C are precipitated in the coating [26]. The EDS results of the typical zones marked A, B, C, D, E, F, G and H in Fig. 1 are listed in Table 2. As shown in Fig.1a, at 100%WC, irregular shaped WC particles, numerous coarse carbides and a few eutectics of the nanocarbides enclosed in the coarse carbide boundary are formed in the clads, which mainly consist of hypereutectic structures including primary columnar dendrites with O-, W- and C-based phases(marked A) being detected amongst the white areas, and eutectics with O-, Fe-, W- and C-rich phases (marked B) being formed in the darker regions. This is due to the different temperature gradients between the white and dark areas, resulting in unmelted WC and surrounding precipitates in the melt pool. EDS analysis showed that at 100 % WC content, there was less variation of tungsten carbide in the primary dendrites compared to the interdendritic eutectic region. As shown in Fig. 1 b, at 50 % WC-50 % Co, the microstructures of the WC particles with interfaces, several micro-cracks, W-based fishbone-dendritics and white-plates carbides as well as eutectic carbides are detected in the molten zone. A dark-white area surrounding the WC particles with a thickness of about 3 – 8 um was formed. The direction of the primary dendrites were perpendicular to the unmelted WC particles at the edges was grown, which were largely thicker than that produced by other fractions. Most of the second dendritics are asymmetric. The inhomogeneous distribution of the eutectic phases with different shapes is found and more micro-cracks existed in the matrix, which was generated in the grain boundaries between the eutectic clusters. In addition, EDS analysis shows the contents of Fe, O and C in the blocky carbide with the point marked D being much higher than that in the dendritic and herringbone carbides marked C, whereas the W contents in the herringbone and dendritic carbides are higher than that in the blocky carbides. The grain boundaries were a weaker zone and therefore the cracks easily formed and propagated. Additionally, for the SEM observation from 50 % WC-50 % Co composites, the cracks were easier to generate in the eutectics than the WC particles. As shown in Fig.1c, based on the SEM micrographs and EDS analysis, the microstructures of 50 % Ni-50 % WC are not fully grown and finer structures are also found. Several sharp and blocky interfaces are grown outward from the WC particles and slighter long-bone carbides are distributed almost randomly in the molten zone, with many Ni-based eutectics in the grey zone. The blocky structures contained a high concentration of W and some fraction of the Ni, and the slighter long-bone carbides contained large amounts of W (66.052 %) and Ni (22.511 %), and a lower fraction C of 1.464% as marked E, in addition, Ni-based eutectics contained large amounts of W (54.676 %) and Ni (31.520 %), respectively, and a lower fraction C (1.867 %) as marked F. Fig. 1 c shows the greater the content of the WC particle marked E, the higher the content of Ni particle marked F will be in the case of 50 % Ni-50 % WC blends during laser cladding. Most of the precipitated carbides with faceted shapes were observed in the composites and the second carbides were seen in the high W contents. However, the grain size of the carbides in the 50 % WC-50 % Ni clads was smaller than that of the others. This may be due to the low free-formation enthalpy of WC, resulting in it being easily dissolved in the Ni-based molten pools.

Table 1. The design in terms of the original variables and the observed response by laser cladding

No. of tests	Pseudo component			Proportion of alloy, wt.%			Residual stress	Vicker hardness	Wear volume
	X1	X2	X3	A-WC	B-Co	C-Ni	MPa	HV	$10^{-4c}mm^3$
1	1/3	1/3	1/3	33.33	33.33	33.33	-177.76	526	3.66
2	1	0	0	100	0	0	-231.21	1200	0.925
3	0	0	1	0	0	100	137	115	168.7
4	1/2	0	1/2	50	0	50	41.6	568	4.14
5	1/6	1/3	1/6	16.67	16.67	66.67	-94	438	9.6
6	0	1/2	1/2	0	50	50	87.81	255	6.91
7	1/2	1/2	0	50	50	0	-219.07	612	1.19
8	0	1	0	0	100	0	-136.52	318	40.4
9	1/6	1/3	1/6	16.67	66.67	16.67	-68.98	329	9.4
10	1/3	1/6	1/6	66.67	16.67	16.67	-94.36	711	32.2

As shown in Fig. 1 d, much fewer partial WC particles as well as blocky carbides are discovered in the molten pool, and the amount of WC particles significantly decreases when both the Co and Ni alloys are mixed with WC powders. The microstructure of the 66.7 % WC-16.7 % Ni-16.7 % Co is transformed from dendritic morphologies into coarse equiaxed shape during laser cladding, where the precipitated carbides advance in the form of the facet solid/liquid interface and grow into blocky carbides. The EDS of the 66.7 % WC-16.7 % Ni-16.7 % Co is illustrated in Fig. 1 d marked G and H.

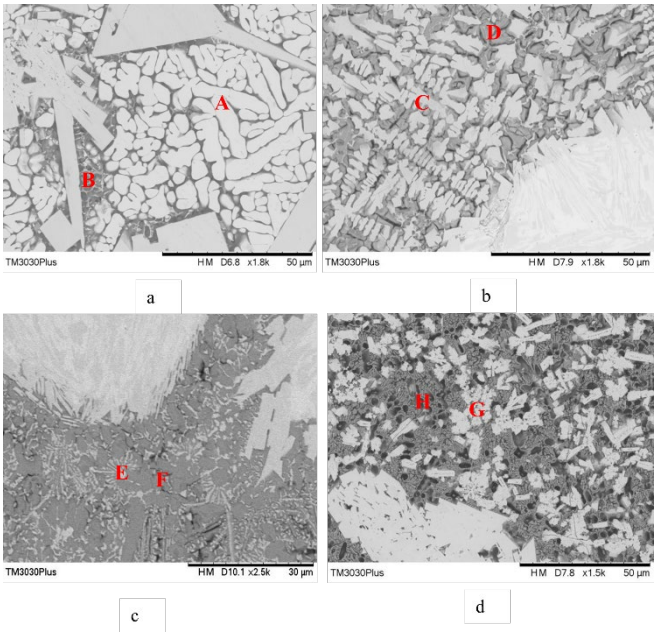

Fig. 1. The SEM images of WC with mixed Co/Ni ratio with red marks, indicating the alloy composition in Table 2 including: a – trial 2 of 100 % WC; b – trial 7 of 50 % WC-50% Co; c – trial 4 of 50 % WC-50 % Ni; d – trial 10 of 66.7 % WC-16.67 % Co-16.67 % Co

The content of the W-based carbides in the white, marked G, is much greater than that of blocky carbides, as well as the Co, Ni and O elements also appear in the dark area marked H. There is no noticeable presence of cracks, porosities and other metallurgical defects. Local decomposition of the WC particles was obviously present around the interior and a cluster carbide is detected in the white area, as well as many finer Co/Ni carbides being noted in the dark area during WC/Co/Ni clads. The structural distribution of the WC/Co/Ni clads is unevenly dispersed across the molten zone. Combining Table 2 with Fig. 1, various types of carbide with different blend fractions were observed in the laser-clad WC/Co/Ni coatings, where undissolution of WC particles, dissolution of WC particles, the fish-bone, blocky, needle-like and faceted carbides were found to be distributed almost randomly in the molten pools.

4.2. Distribution of residual stress and crack morphology analysis

To control cracking generated within the clad, an understanding of the nature of residual stress behaviors in laser clads is needed. The surface residual stresses determined by X-ray diffraction are only concerned with the WC/Co/Ni welds, as shown in Fig. 2. The complete center composite with experimental data is conducted in Table 2, which presents the residual stress of the clads through the values of the slope of the plot according to the pattern of fitting a Gauss function to a measured peak by X-ray diffraction in Fig. 2 a, to calculate the residual stress [27]. The distribution of measured residual stresses is shown in Table 2, where the compressive stresses mostly range between -231 MPa and -69 MPa and tensile stresses range from 42 MPa to 137 MPa with different ingredient percentages being observed. As shown in Fig. 2 b, the pattern of fitting a Gauss function with four blend ratios for the WC/Co/Ni welds is observed. The residual stress behavior mainly depends on the percentages of ingredients in the ceramic- matrix composite coatings. Overall, the compressive stress values for the three powders with WC, Co and Ni blends are found. The 100 %WC has higher residual stress in the welded clads, while higher tensile stresses at 100 % Ni are seen during the overall tests [28, 29]. The residual stress of 50 % WC-50 % Ni was markedly decreased, which also reflected the superior structures in the Ni-based WC composites. That is, the micro-stresses were markedly reduced and thereby the crack susceptibility was suppressed. It is reasonable to believe the higher stress of each for the WC/Co/Ni welds, except trial 1 and trial 7 could be found, while the influence of WC with the additive of Co alloys on residual stresses is unknown. The crack morphology is shown in Fig. 2 c, when for the content of 100 % WC, the microcracks at residual stress values of -231.21 MPa were randomly distributed around molten zones. Cracks in the brittle WC particles occur in which those stresses appear to exceed the yield stress of the WC due to high stress concentration.

Table 2. Chemical composition analysis with atomic concentrations of the weight percentages of WC/Co/Ni alloys in the WC (Co, Ni) clads with the marked location in Fig. 1

No. of trials	Atomic concentration, %								Analysis location
	C	O	S	Fe	Co	Ni	Cu	W	
2	3.112	1.709	0.035	2.450	0.229	0.486	0.263	91.72	A
2-1	1.317	4.365	0.106	2.933	0.245	0.000	0.298	90.735	B
7	1.679	1.111	0.077	0.951	22.266	1.000	0.425	72.490	C
7-1	4.392	7.950	0.185	17.917	19.466	0.000	0.491	49.599	D
4	1.464	6.662	0.108	2.403	0.515	22.51	1.274	66.052	E
4-1	1.867	8.392	0.156	3.076	0.000	31.520	0.314	54.676	F
10	0.990	1.743	0.068	0.709	9.018	3.463	0.000	84.009	G
10-1	1.740	12.655	0.059	3.367	28.916	5.807	1.185	46.271	H

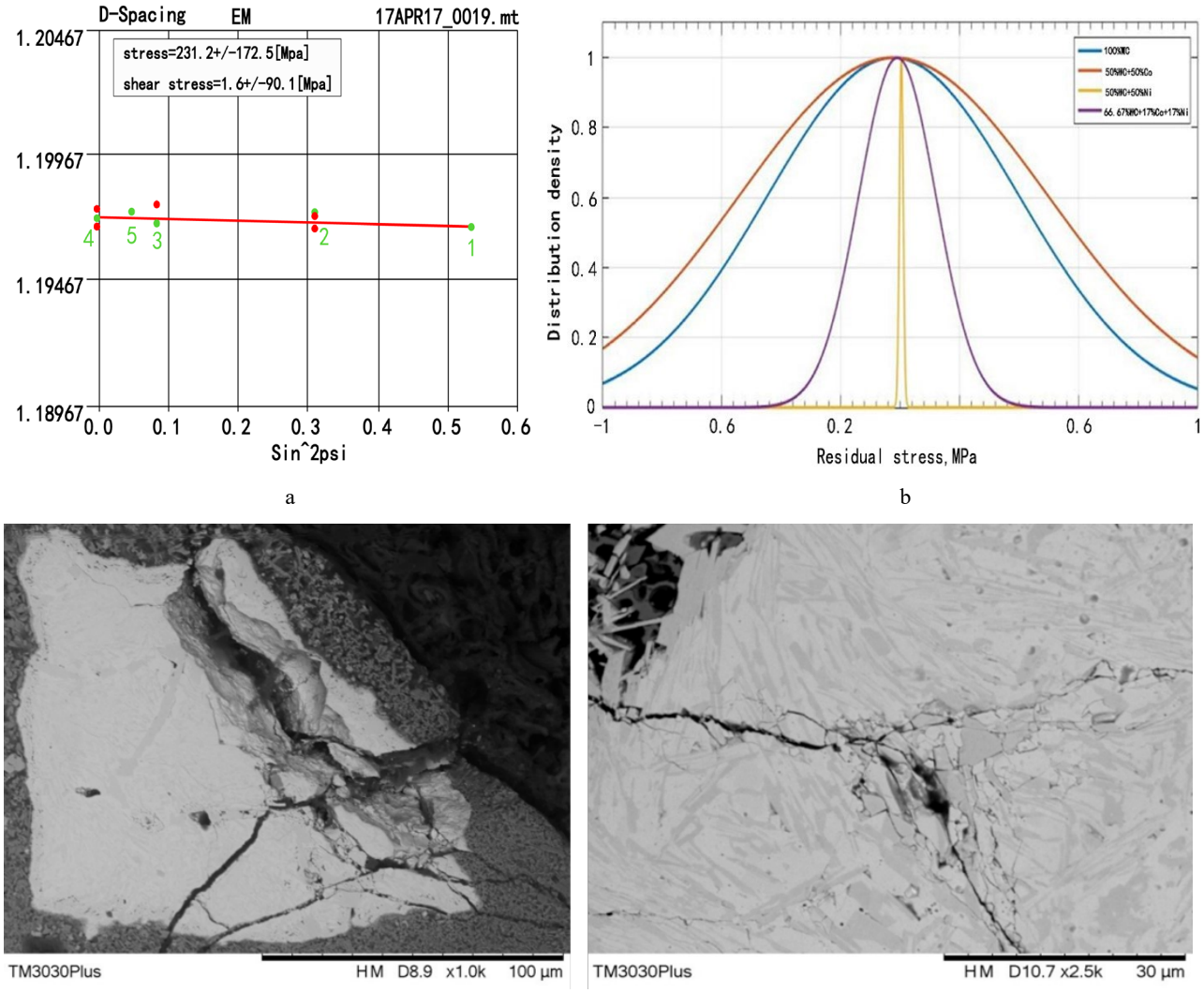

Fig. 2. The measured residual stresses of the d-sin2ψ pattern: a – the pattern of fitting a Gauss function; b – the residual stresses with four blend ratios for the WC/Co/Ni welds and microstructural evolution with crack formations; c – 100 % WC; d – 50 % WC-50 % Co

Additionally, as shown in Fig. 2d, at -219 MPa residual stress, the macro-cracks originating from the free-surface of the clads and propagated through the WC particle in branches and also the fractured cracks are effectively broken down into fine debris in the interior of the WC particles in the 50 % WC-50 % Co composite welds. The residual stress behaviors may be due to the effects of the combinations of thermal stress and transformation stress from the volume variations associated with phase transformation. However, crack propagation in a transverse direction proceeds due to the higher thermal gradient associated with rapid solidification in the cladding welds. Accordingly, it may be concluded the presence of residual stress due to a large volume fraction of carbides is responsible for crack formation.

4.3. Microhardness analysis

To understand the influence of different blend fractions of WC/Co/Ni alloys on laser-clad welds, the microhardness of the cross-section profiles was evaluated with the depth from the surface of the clads. Fig. 3 a shows the microhardness distributions with 100 % WC, 50 % WC-50 % Co, 50 % WC-50 % Ni and 66.7 % WC-16.7 %Co-16.7 % Ni welds, respectively are plotted. The distribution of the microhardness of the WC/Co/Ni deposits is significantly different using a blend of weight fractions of WC/Co/Ni alloys.

The hardness of the molten pools is 1200 ± 267 HV for 100 WC, 632 ± 76 HV for 50 % WC-50 % Co, 588 ± 84 HV for 50 % WC-50 % Ni and 641 ± 57 HV for 66.7 % WC-16.7 % Co-16.7 % Ni alloys, respectively. The additive of 100 % WC welds enhanced the microhardness by almost five times with higher hardness values in all trials, while in the case of 100 % Co or 100 % Ni, the hardness values of each trial at 318 HV or 115 HV are obviously lower in all tests. The results indicate the higher WC content on the microhardness of the coatings has an obvious effect. This higher hardened behavior can be attributed to large amounts of hard WC carbides in the molten pools. Fig. 3 b shows the distribution of iso-hardness contour at various blend ratios of the WC/Co/Ni welds. The microhardness of the solidified zone is not uniformly distributed in the WC/Co/Ni welds, which vary from 300 HV to 1400 HV. The difference in microhardness is attributed to the

development of a blend of different fractions consisting of different carbides dispersed in the laser clads. From the SEM observation of the microstructure and microhardness values, the higher hardness levels of the molten zone associated with the fine microstructures are clearly visible for the cladding WC/Co/Ni clads due to the production of rapid solidification in the molten zone. On the other hand, the microstructures are coarser and the microhardness is lower. The decrease in hardness with high Co/Ni alloys is attributed to the WC content with fewer hard carbides and coarser grain size.

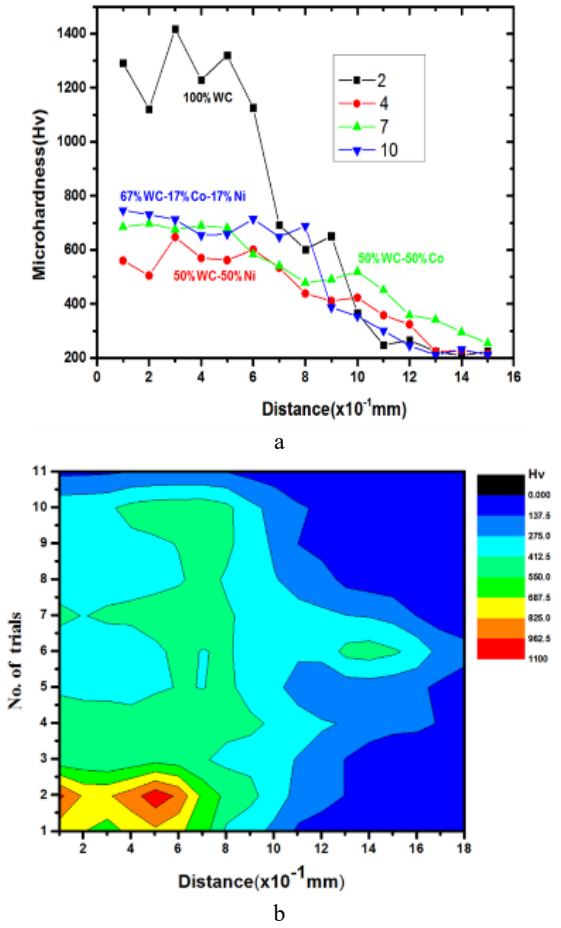

Fig. 3. A comparison of microhardness between various fractions of WC/Co/Ni alloys: a – microhardness distribution of the depth from the surface with four different blends; b – iso-hardness contours of all the trials

4.4. Fractured morphology and wear behavior analysis

Wear tests with different weight percentages of WC/Co/Ni welds were carried out and the worn morphologies were checked by scanning electron microscopy. The graphs in Fig. 4 show the results of wear tests for four different blend ratios during WC/Co/Ni coatings, whereby the various curve patterns of wear in the right upper corner area can be observed. The distributions of measured wear volume prepared by each weight percentage of mixtures include 100 % WC, 50 % WC-50 % Co, 50 % WC-50 % Ni and 66.7 % WC-16.7 % Co-16.7 % Ni are 9.0×10^{-5} mm^3, 1.19×10^{-4} mm^3, 4.14×10^{-4} mm^3 and 32.2×10^{-4} mm^3, respectively, where they appear to be three times lower than the substrate [30 – 34]. The abrasive wear of the 100 % WC-based cladding layer was marked much more than that of other blend ratios. Fig. 4 a shows a 3D topography profile of the wear track with the SEM micrograph of the 100 % WC welds. It can be seen that a worn surface with irregular but shallow unknown grooves is found on the worn track. the typical abrasive mechanism, and the curves of the scar area in each cross-section are obtained as marked in the right upper corner of Fig. 4 a with 0.18 um wear depth. The unmelted WC particles having good interfacial bonding attached to the matrix of the cladding layer are discovered in Fig. 4 b, where few dark pits existed within the WC. In addition, the results of the EDS analysis shown in Fig. 4 b show the worn surfaces were rich in W, O, C and Fe, and large amounts of W. The iron fragments contacted by the counterpart are carried into the wear track that is oxidized which forms iron oxides in the brittle region.

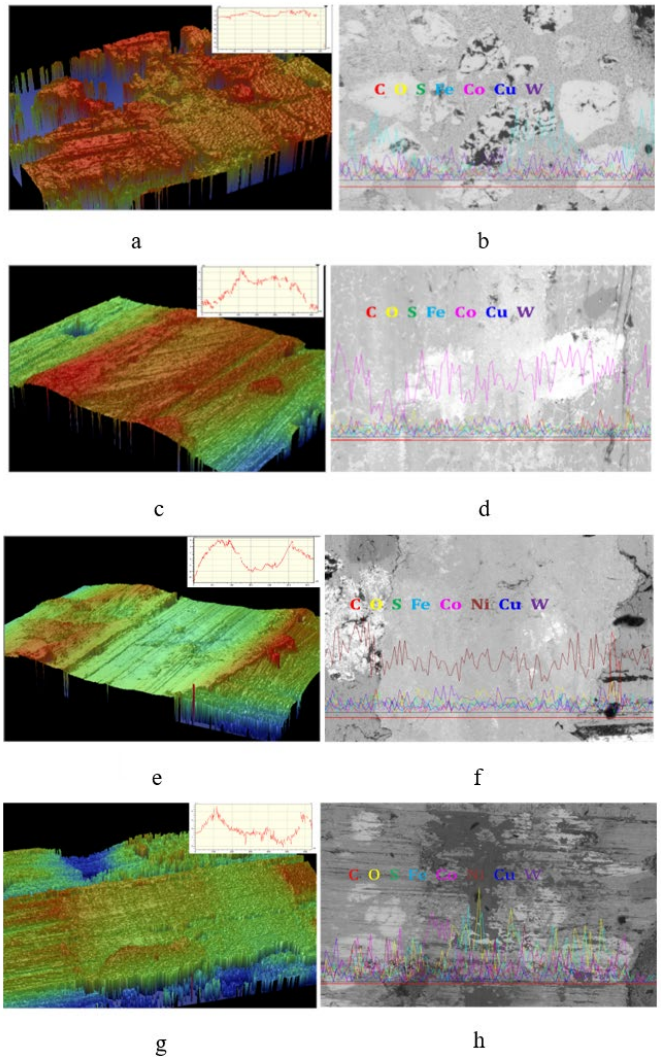

Fig. 4. The 3D topography mapping and SEM micrographs with EDS patterns of the corresponding wear scars of the worn surfaces: a – 100 % WC; b – 100 % WC; c – 50 % WC-50 % Co; d – 50 % WC-50 % Co; e – 50 % WC-50 % Ni; f – 50 % WC-50 % Ni; g – 66.7 % WC-16.7 % Co-16.7 Ni; h – 66.7 % WC-16.7 % Co-16.7 Ni respectively, of WC/Co/Ni coatings

Thus, the WC carbides are not easily removed from the matrix due to the obvious dispersion strengthening effect of

the hard carbides. The worn 3D surface morphology shown in Fig. 4 c is very similar to that of the worn graph, as observed in Fig. 4 a. EDS analysis and fractured micrographs are shown in Fig. 4 d. Some furrows, fewer pores and large amounts of unfastened small WC particles around the matrix are observed, and a white area, which is left after micro cutting, as well as local plastic deformation in the worn surface are visible, indicating an abrasive-adhesive mechanism. This phenomenon mainly occurs because the wear mechanism is generated by a combination of microcutting with brittle debonding wear. It highlights the presence of W, O, C and Fe, and large amounts of Co. As shown in Fig. 4 e, based on the 3-D surface mapping of the worn tracks, large furrows, pits and deep grooves in the worn track are marked. In addition, the results of EDS analysis shown in Fig. 4 f show the worn surfaces were rich in W, O, C and Fe, and large amounts of Ni. The worn surface of the 50 % WC-50 % Ni coatings shows the adhesive wear mechanism with severe plastic deformation and severe spalling of Ni binders, where the worn surface becomes comparatively smooth and some spalling patterns are also seen. Contrary to the 50 % WC-50 % Co weld, signs of both adhesive and abrasive wear appear and fewer furrows are found on the worn surface during running-in. Thus, the cladding welds exhibit a lower wear resistance due to low binding capacity. In the case of 66.7 % WC-Co 16.7 %-Ni 16.7 %, the 3D topography mapping of the corresponding wear scars of the worn surfaces in Fig. 4 g shows deep grooves with a smooth zone and wide continuous tracks on the worn surface. This is reflected in Fig. 4 h with a wear depth of 0.8 um. The wear mechanism of the worn surface shows signs of adhesive wear and severe plastic deformation, in which a lot of WC particles are pulled out of the matrix due to the large deformation and soft Co-Ni oxides in the matrix that stick to the matrix during wear. In addition, the results of the EDS analysis shown in Fig. 4 h show the worn surfaces were rich in Co, Ni, W and Fe, and large amounts of O. The welds become softened and large amounts of deformations occur. The soft Co/Ni oxidation layers with weak properties are detached during adhesive wear. This situation causes the local binder oxidized phases to become softened, and thereby the soft matrix cannot resist the wear when contacting the high hard countpart during running-in. In such a case, the wear resistance of 66.7 % WC-Co 16.7 %-Ni 16.7 % was the worst of the WC/Co/Ni coatings. From observation of the SEM micrograph of the worn surface along with the chemical composition analysis, the results showed the concentration of WC in the welds significantly affects the wear mechanism. Accordingly, increasing the percentage of additives of Co/Ni on WC can not effectively improve the wear resistance of laser-clad joints, while avoiding cracking. However, by increasing the percentage of Co/Ni on WC, adhesive wear is more significant than abrasive wear. The wear resistance of the laser-clad welds is improved by the high content of WC particles in the welds.

4.5. Empirical models of mechanical properties

The design and observed responses are shown in Table 2 with all of the responses including residual stress, microhardness and wear volume losses for the laser-clad welds. The results for all responses supported by regression with experimental design are analyzed using SPSS20 [35]. An analysis of variance is given in Table 3. A simplex-centroid design for three components is adopted to study the quality of the responses for laser-clad welds.

Table 3. Summarizes the ANOVA for linear of hardness, and reduced special quartic mixture models of residual stress and wear volume

Mechanical properties	Source	Sum of squares	df	Mean square	F value	p-value Prob > F
Residual stress	Model	1.48E+05	6	24638.11	11.59	0.035
	Linear Mixture	1.08E+05	2	53845.03	25.33	0.0132
	AB	831.72	1	831.72	0.39	0.576
	AC	5586.79	1	5586.79	2.63	0.2035
	BC	7185.02	1	7185.02	3.38	0.1633
	ABC^2	32264.41	1	32264.41	15.18	0.0300
	Residual	6378.36	3	2126.12		
	Cor Total	1.54E+05	9			
Micro-hardness	Model	7.66E+05	5	1.53E+05	11.9	0.0163
	Linear Mixture	7.46E+05	2	3.73E+05	28.94	0.0042
	AB	13666.76	1	13666.76	1.06	0.3612
	AC	1038.95	1	1038.95	0.081	0.7905
	BC	5813.43	1	5813.43	0.45	0.5386
	Residual	51535.59	4	12883.9		
	Cor Total	8.18E+05	9			
Wear volume	Model	23632.44	7	3376.06	87.12	0.0114
	Linear Mixture	9582.9	2	4791.45	123.65	0.008
	AB	211.19	1	211.19	5.45	0.1447
	AC	4302.09	1	4302.09	111.02	0.0089
	BC	6313.08	1	6313.08	162.92	0.0061
	A^2BC	2869.99	1	2869.99	74.06	0.0132
	ABC^2	1362.09	1	1362.09	35.15	0.0273
	Residual	77.5	2	38.75		
	Cor Total	23709.94	9			

In all cases, linear, quadratic, quartic and cubic mixture models are tested. Table 3 shows the model p-values of 0.035 of residual stress for the linear model, 0.0163 of microhardness for the special quartic mixture and 0.0114 of wear volume losses for the special quartic mixture model, respectively, successfully achieved, which are less than 0.05, indicating the models obtained fitting significance. The result is confirmed by computing the determination coefficients (R^2) of the above models, which were 0.958, 0.912 and 0.996, respectively, meaning the models fitted well. This statistic indicates the linear model for microhardness and reduced special quartic mixture model of both residual stress and wear volume losses for the laser-clad WC/Co/Ni welds are superior to other models as quadratic and cubic mixture models. Accordingly, these models could be used to forecast the quality of the responses for a laser-clad weld. In other words,the canonical forms of the linear and special quartic mixture model for the cladding WC/Co/Ni welds are conducted, and the canonical form of the mixture models for the three responses such as residual stress (Y_1), microhardness (Y_2) and wear volume (Y_3) are as follows:

$$Y_1 = -249.09\ A - 128.12\ B + 107.98\ C - 134.26\ AB + 358.15\ AC + 406.16\ BC - 14440.47\ ABC^2 \quad R^2 = 0.9585; \tag{2}$$

$$Y_2 = 1153.38\ A + 296.47\ B + 144.65\ C - 519.64\ AB - 143.27\ AC + 338.91\ BC \quad R^2 = 0.912; \tag{3}$$

$$Y_3 = -0.029\ A + 42.38\ B + 167.75\ C - 69.99\ AB - 320.65\ AC - 382.66\ BC + 5143.32\ A^2BC - 3543.30\ ABC^2 \quad R^2 = 0.996. \tag{4}$$

Based on the analysis of variance, the ternary contour plots of the three-component blends on mechanical properties were generated based on Eq. 2 – Eq. 4, as shown in Fig. 5, where the oval shape of isoline reflects an interaction index, but is contrary to the round shapes. The effects of the interaction of the components on the models differ. It can be seen the residual stresses for the linear model have no interaction effect, while both microhardness and wear volume losses for the quartic mixture model have significant interactive impacts. As shown in Fig. 5 a, the ternary contour plots illustrate the effects of the mixture component and their interactions on the residual stress behaviors. Comparing the previous result [36], there seems to be a little difference, but the predicted results are consistent. This is mainly attributed to the multiple quality characteristics in this study. The lowest yields are obtained by higher Ni and lower WC/Co contents, whereas high contents of WC and Co could produce much larger yields. In other words, Ni alloys favored the reduction of the residual stresses, because high stress concentrations could be relaxed by Ni binders mixed with WC alloys. It is clear from the figure that when the contour comes near the zero iso-line in the special quartic mixture, the Ni additive on WC significantly affects the residual stress patterns. The ternary contour plots in Fig. 5 b show the microhardness value increased remarkably toward the vertex of the WC alloys. The highest yield on the contour graph is seen to take place at the high WC proportion of all three-component combinations. Increasing the Ni alloys for the WC/Co/Ni mixture provided a lower increment in the hardness value of the laser-clad welds compared to the higher Co and WC additives because Ni alloys are less hard than the others. As shown in Fig. 5 c, the special quartic mixture of each component, and the interaction of both WC-Ni and Co-Ni alloys significantly affected the wear volume losses of the laser-clad welds. It increased toward the vertex of Ni alloys, while it decreased toward the vertex of WC alloys. The relatively lower increment of WC alloys compared to nickel alloys results in reduced wear, which may be due to the wettable nickel alloy phase which surrounds the high hardness carbide in the melt zone.

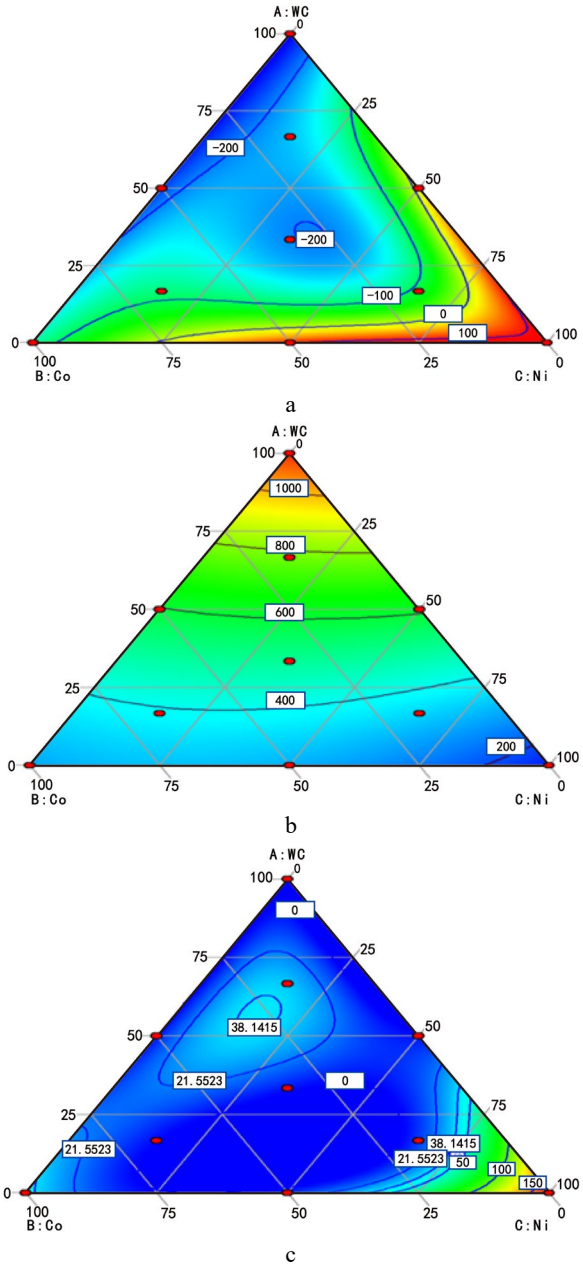

Fig. 5. Ternary contour plot of three components for various models, accounting for the effect of the individual and mixture on the yields: a – residual stress; b – microhardness; c – wear volume

Fig. 6 shows the overlay plots of the different models predicted yield in terms of microhardness, wear volume losses and residual stress as a function of the WC, Co and Ni proportions of WC/Co/Ni blended welds in the same operating conditions, in which the optimal blend fraction of WC, Co and Ni mixture was found to achieve the highest desirability function. According to Eq. 2 – Eq. 4 and analysis of the contour plots in Fig. 5, Fig. 6 shows the contour patterns by superimposing the contour with three different yields being overlaid and the overlay contour patterns finding the optimal zone.

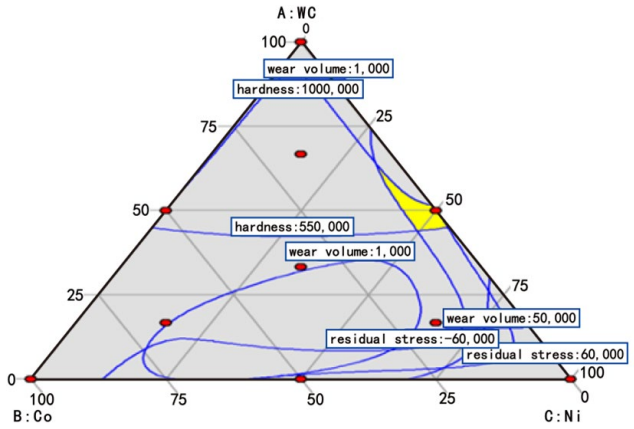

Fig. 6. Response surface contour with overlaid plots of three different models for predicted yield in terms of microhardness, wear volume losses and residual stress as a function of the WC, Co and Ni proportions of WC/Co/Ni coatings

Based on the overlay plots, the most desirable quality of cladding WC/Co/Ni coatings is obtained, indicating the feasible solution with yellow marked regions is found in the overlaid contour plots of the yields. In addition, as shown in Table 4, nine different optimal solutions with function desirabilities were tested. The optimal blend ratio of the mixture was obtained and several of the highest desirability functions are desirable when the WC content is at 52 – 58 %, the Co content is at 1 – 10 % and the Ni content is at 38 – 47 %. By conducting the validation experiments, a better desirability function is positively achieved. As the optimal plot depicts in Fig. 6, the optimum proportions of the mixture were 54 % WC, 8 % Co and 38 % Ni. Additionally, the predicted responses for residual stress, microhardness and wear volume losses, respectively, were 729.29 HV, -80.57 MPa and 6.779×10^{-4} mm^3 with a high composite desirability of one However, the quality characteristics of the cladding WC/Co/Ni welds are modified by tuning the blend fraction based on the experimental study's criteria. On the other hand, the microstructural evolution, residual stress, microhardness and wear behaviors of a clad were controlled using a multi-objective superimposed optimization technique. Overall, for the cladding WC/Co/Ni welds, the improvements in microstructural evolution, crack susceptibility and mechanical properties were closely related to the various weight percentages of mixture of the WC/Co/Ni powders. The results of this study were compared with the findings of other researchers [37, 38], and the predicted results fell into a feasible zone of solutions, which is a consistent result. However, the results of this study provide a comprehensive solution for the optimization among multiple elements and properties.

5. CONCLUSIONS

This study achieved a reliable mixture-design approach for ceramic-matrix composites in additive manufacturing processes developed with a mixture of Co, Ni and WC powders that were applied to find suitable blend ratios to enhance laser-clad quality on the yields including microstructural evolution, microhardness, wear resistance and residual stress behavior of a laser clad. The following conclusions can be drawn:

1. From the observation of EDS analysis, in the case of 50 % WC-50 % Co, the microstructures of WC particles with interfaces, several micro-cracks, fishbone-dendritics, blocky carbides and Co-based eutectic carbides are detected. In addition, the microstructures of 50 % WC-50 % Ni with slight dendritics and smaller eutectics are found, and several sharp and blocky interfaces are grown outward from the WC particles.
2. The distribution of measured residual stresses including compressive stress is mostly between -231 MPa and -69 MPa and tensile stresses ranging from 42 MPa to 137 MPa at different ingredient percentages are observed. The residual stress behaviors may be due to producing the effects of the combinations of thermal stress and transformation stress from the volume variations associated with phase transformation.
3. An SEM micrograph of the worn surface along with the chemical composition analysis showed the concentration of WC in the cladding welds significantly affects the wear mechanism for the cladding WC/Co/Ni welds. It is found increasing the percentage of Co/Ni on WC, adhesive wear is more relevant than abrasive wear decrease.

Table 4. The desirability of the functions with different optimal solutions including blend fractions and mechanical propertie of a clad

No. of tests	WC	Co	Ni	Hardness, HV	Residual stress, MPa	Wear volume, 10^{-4}mm^3	Desirability	
1	52	1	47	701.142	-55.7300	1.37257	1	
2	52	10	38	712.940	-79.9114	9.3237	1	
3	55	4	40	740.767	-76.2139	0.987836	1	
4	52	7	42	705.264	-69.6043	4.69443	1	
5	52	8	40	712.973	-75.2388	6.41474	1	
6	55	6	39	738.974	-79.4693	3.75444	1	
7	53	5	42	715.803	-69.0365	2.59637	1	
8	58	5	37	766.163	-87.8011	2.91174	1	
9	54	8	38	729.293	-80.5767	6.77998	1	Selected

4. The addition of Co/Ni to the WC increase in the coatings decreases the microhardness of the cladding WC/Co/Ni welds, and does not improve residual stress, while constraining crack generation. The lower residual stresses associated with good bonding between Co/Ni and WC are obtained at 50 % Ni-50 % WC.
5. Based on the overlay plots, a desirable quality of cladding WC/Co/Ni coatings is obtained and a feasible solution with a marked region is achieved when the WC content is 52 – 58 %, the Co content is 1 – 10 % and the Ni content is 38 – 47 %.

Further, the predicted responses for residual stress, microhardness and wear volume losses, respectively were 729.29 HV, -80.57 MPa and 6.779×10^{-4} mm^3 with a high composite desirability of one. Overall, the microstructural evolution and defects, hardness and wear behaviors of a clad were effectively controlled using a multi-objective superimposed optimization technique. However, the results of this study provide a comprehensive solution for optimizing the relationship between multiple elements and properties through mixture design.

REFERENCES

1. **Babu, P.S., Basu, B., Sundararajan, G.** Processing–Structure–Property Correlation and Decarburization Phenomenon in Detonation Sprayed WC–12Co Coatings *Acta Materialia* 56 (18) 2008: pp. 5012 – 5026. https://doi.org/10.1016/j.actamat.2008.06.023
2. **Zhu, Y.C., Ding, C.X., Yukimura, K., Xiao, T.D., Strutt, P.R.** Deposition and Characterization of Nanostructured WC–Co Coating *Ceramics International* 27 (6) 2001: pp. 669 – 674. https://doi.org/10.1016/S0272-8842(01)00016-5
3. **Huang, Y., Zeng, X.** Investigation on Cracking Behavior of Ni-based Coating by Laser-Induction Hybrid Cladding *Applied Surface Science* 256 (20) 2010: pp. 5985 – 5992. https://doi.org/10.1016/j.apsusc.2010.03.106
4. **De Oliveira, U., Ocelík, V., De Hosson, J.T.M.** Residual Stress Analysis in Co-Based Laser Clad Layers by Laboratory X-rays and Synchrotron Diffraction Techniques *Surface and Coatings Technology* 201 (3 – 4) 2006: pp. 533 – 542. https://doi.org/10.1016/j.surfcoat.2005.12.011
5. **Sun, G., Zhou, R., Lu, J., Mazumder, J.** Evaluation of Defect Density, Microstructure, Residual Stress, Elastic Modulus, Hardness and Strength of Laser-deposited AISI 4340 Steel *Acta Materialia* 84 2015: pp. 172 – 189. https://doi.org/10.1016/j.actamat.2014.09.028
6. **Montay, G., Cherouat, A., Nussair, A., Lu, J.** Residual Stresses in Coating Technology *Journal of Materials Science and Technology* 20 2004: pp. 81 – 84.
7. **Farahmand, P., Kovacevic, R.** Laser Cladding Assisted with an Induction Heater (LCAIH) of Ni–60 % WC Coating *Journal of Materials Processing Technology* 222 2015: pp. 244 – 258. https://doi.org/10.1016/j.jmatprotec.2015.02.026
8. **Afzal, M., Khan, A.N., Mahmud, T.B., Khan, T.I., Ajmal, M.** Effect of Laser Melting on Plasma Sprayed WC-12 wt.% Co Coatings *Surface and Coatings Technology* 266 2015: pp. 22 – 30. https://doi.org/10.1016/j.surfcoat.2015.02.004
9. **Kapadia, P., Davies, C., Pirling, T., Hofmann, M., Wimpory, R., Hosseinzadeh, F., Dean, D., Nikbin, K.** Quantification of Residual Stresses in Electron Beam Welded Fracture Mechanics Specimens *International Journal of Solids and Structures* 106 2017: pp. 106 – 118. https://doi:10.1016/j.ijsolstr.2016.11.028
10. **Zhong, M., Liu, W., Yao, K., Goussain, J.C., Mayer, C., Becker, A.** Microstructural Evolution in High Power Laser Cladding of Stellite 6+ WC Layers *Surface and Coatings Technology* 157 (2 – 3) 2002: pp. 128 – 137. https://doi.org/10.1016/S0257-8972(02)00165-2
11. **Zhong, M., Liu, W.** Microstructure Evolution of Stellite 6+WC by High Power Laser Cladding *Acta Metal* 38 (5) 2002: pp. 495 – 500. https://doi: 10.3321/j.issn:0412-1961.2002.05.010
12. **Zhong, M., Liu, W., Zhang, Y., Zhu, X.** Formation of WC/Ni Hard Alloy Coating by Laser Cladding of W/C/Ni Pure Element Powder Blend *International Journal of Refractory Metals and Hard Materials* 24 (6) 2006: pp. 453 – 460. https://doi.org/10.1016/j.ijrmhm.2005.09.002
13. **Han, J.C., Jafari, M., Park, C.G., Seol, J.B.** Microstructure-Property Relations in WC-Co Coatings Sprayed from Combinatorial Ni-plated and Nanostructured Powders *Materials Characterization* 129 2017: pp. 207 – 216. https://doi.org/10.1016/j.matchar.2017.05.005
14. **Zhou, S., Zeng, X., Hu, Q., Huang, Y.** Analysis of Crack Behavior for Ni-based WC Composite Coatings by Laser Cladding and Crack-Free Realization *Applied Surface Science* 255 (5) 2008: pp. 1646 – 1653. https://doi.org/10.1016/j.apsusc.2008.04.003
15. **Lee, C., Park, H., Yoo, J., Lee, C., Woo, W., Park, S.** Residual Stress and Crack Initiation in Laser Clad Composite Layer with Co-based Alloy and WC+ NiCr *Applied Surface Science* 345 2015: pp. 286 – 294. https://doi.org/10.1016/j.apsusc.2015.03.168
16. **Liu, C.W., Jean, M.D., Wang, Q.T., Chen, B.S.** Optimization of Residual Stresses in Laser-Mixed WC(Co, Ni) Coatings *Strength of Materials* 51 (1) 2019: pp. 95 – 101. https:// doi:10.1007/ s11223-019-00054-z
17. **Bai, Y., Yang, Y., Xiao, Z., Zhang, M., Wang, D.** Process Optimization and Mechanical Property Evolution of AlSiMg 0. 75 by Selective Laser Melting *Materials & Design* 140 2018: pp. 257 – 266. https://doi.org/10.1016/j.matdes.2017.11.045
18. **Fernández, M.R., García, A., Cuetos, J.M., González, R., Noriega, A., Cadenas, M.** Effect of Actual WC Content on the Reciprocating Wear of a Laser Cladding NiCrBSi Alloy Reinforced with WC *Wear* 324 2015: pp. 80 – 89. https://doi.org/10.1016/j.wear.2014.12.021
19. **Zafar, S., Sharma, A.K.** Investigations on Flexural Performance and Residual Stresses in Nanometric WC-12Co Microwave Clads *Surface and Coatings Technology* 291 2016: pp. 413 – 422. https://doi.org/10.1016/j.wear.2014.12.021
20. **Khalilian, H., Semnani, A., Haddadi, H., Nekoeinia, M.** Multi-Response Optimization of a Hydraulic Oil Formulation by Mixture Design and Response Surface Methods *Journal of Tribology* 138 (2) 2016: pp. 021801. https://doi.org/10.1115/1.4031397
21. **Khaskhoussi, A., Calabrese, L., Bouhamed, H., Kamoun, A., Proverbio, E., Bouaziz, J.** Mixture Design Approach to Optimize the Performance of TiO2 Modified Zirconia/Alumina Sintered Ceramics *Materials & Design*

137 2018: pp. 1 – 8.
https:/doi.org/10.1016/j.matdes.2017.10.010

22. **Bai, J., Zuo, W.** Multi-Material Topology Optimization of Coated Structures Using Level Set Method *Composite Structures* 300 2022: pp. 116074.
https://doi.org/10.1016/j.compstruct.2022.116074
23. **Luo, Q., Jones, A.H.** High-Precision Determination of Residual Stress of Polycrystalline Coatings Using Optimised XRD-sin2ψ Technique *Surface and Coatings Technology* 205 (5) 2010: pp. 1403 – 1408.
https://doi.org/10.1016/j.surfcoat.2010.07.108
24. **Dobročka, E., Novák, P., Búc, D., Harmatha, L., Murín, J.** X-ray Diffraction Analysis of Residual Stresses in Textured ZnO Thin Films *Applied Surface Science* 395 2017: pp. 16 – 23.
https://doi.org/10.1016/j.apsusc.2016.06.060
25. **Myers, R.H., Montgomery, D.C., Anderson Cook, C.M.** Response Surface Methodology: Process and Product Optimization Using Designed Experiments. 3rd ed, John Wiley & Sons, Inc., Hoboken, New Jersey. 2009.
26. **Weng, F., Yu, H., Chen, C., Dai, J.** Microstructures and Wear Properties of Laser Cladding Co-based Composite Coatings on Ti–6Al–4V *Materials & Design* 80 2015: pp. 174 – 181.
https://doi.org/10.1016/j.matdes.2015.05.005
27. **Stadelmann, R., Lugovy, M., Orlovskaya, N., Mchaffey, P., Radovic, M., Sglavo, V.M., Grasso, S., Reece, M.J.** Mechanical Properties and Residual Stresses in ZrB2–SiC Spark Plasma Sintered Ceramic Composites *Journal of the European Ceramic Society* 36 (7) 2016: pp. 1527 – 1537.
https://doi.org/10.1016/j.jeurceramsoc.2016.01.009
28. **Zafar, S., Sharma, A.K.** Investigations on Flexural Performance and Residual Stresses in Nanometric WC-12Co Microwave Clads *Surface and Coatings Technology* 291 2016: pp. 413 – 422.
https://doi:10.1016/j.surfcoat.2016.03.009
29. **Wang, C., Jiang, C., Ji, V.** Thermal Stability of Residual Stresses and Work Hardening of Shot Peened Tungsten Cemented Carbide *Journal of Materials Processing Technology* 240 2017: 98 – 103.
https://doi.org/10.1016/j.jmatprotec.2016.09.013
30. **Shu, D., Li, Z., Zhang, K., Yao, C., Li, D., Dai, Z.** In Situ Synthesized High Volume Fraction WC Reinforced Ni-based Coating by Laser Cladding *Materials Letters* 195 2017: pp. 178 – 181.
https://doi.org/10.1016/j.matlet.2017.02.076
31. **Bartkowski, D., Bartkowska, A.** Wear Resistance in the Soil of Stellite-6/WC Coatings Produced Using Laser Cladding Method *International Journal of Refractory Metals and Hard Materials* 64 2017: pp. 20 – 26.
https://doi.org/10.1016/j.ijrmhm.2016.12.013
32. **Yin, S., Ekoi, E.J., Lupton, T.L., Dowling, D.P., Lupoi, R.** Cold Spraying of WC-Co-Ni Coatings Using Porous WC-17Co Powders: Formation Mechanism, Microstructure Characterization and Tribological Performance *Materials & Design* 126 2017: pp. 305 – 313.
https://doi.org/10.1016/j.matdes.2017.04.040
33. **Sui, Y., Yang, F., Qin, G., Ao, Z., Liu, Y., Wang, Y.** Microstructure and Wear Resistance of Laser-Cladded Ni-based Composite Coatings on Downhole Tools *Journal of Materials Processing Technology* 252 2018: pp. 217 – 224.
https://doi.org/10.1016/j.jmatprotec.2017.09.028
34. **Cui, G., Han, B., Zhao, J., Yang, Z.** Microstructure and Tribological Performance of Sulfurizing Layer Prepared on the Laser Cladding Co-based Alloy Coating *Surface and Coatings Technology* 331 2017: pp. 27 – 34.
https://doi.org/10.1016/j.surfcoat.2017.10.005
35. **Lin, B.T., Jean, M.D., Chou, J. H.** Using Response Surface Methodology for Optimizing Deposited Partially Stabilized Zirconia in Plasma Spraying *Applied Surface Science* 253 (6) 2007: pp. 3254 – 3262.
https:// doi: 10.1016/j.apsusc.2006.07.021
36. **Jean, M.D., Lei, P.D., Kong, L.H., Liu, C.W.** Aluminum Nitride Coatings Using Response Surface Methodology to Optimize the Thermal Dissipated Performance of Light-Emitting Diode Modules *AIP Advances* 8 2018: pp. 055106.
https://doi.org/ 10.1063/ 1.5021816
37. **Chen, L., Yu, T., Chen, X., Zhao, Y., Guan, C.** Process Optimization, Microstructure and Microhardness of Coaxial Laser Cladding TiC Reinforced Ni-based Composite Coatings *Optics & Laser Technology* 152 2022: pp. 108129.
https://doi.org/10.1016/j.optlastec.2022.108129
38. **Meng, G., Zhu, L., Zhang, J., Yang, Z., Xue, P.** Statistical Analysis and Multi-Objective Process Optimization of Laser Cladding TiC-Inconel718 Composite Coating *Optik* 240 2021: pp. 166828.
https://doi.org/10.1016/j.ijleo.2021.166828